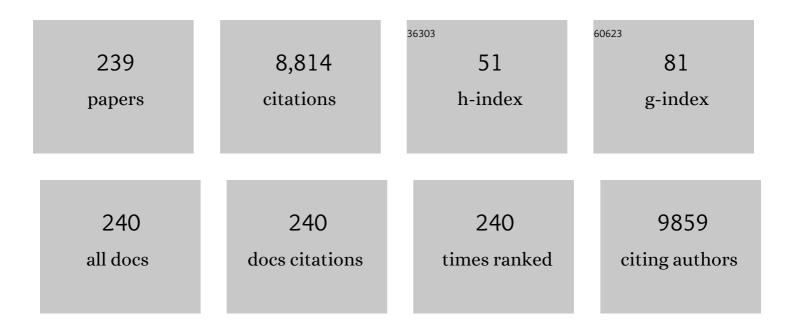
Narsimlu daulatabad

List of Publications by Year in descending order

Source: https://exaly.com/author-pdf/294962/publications.pdf Version: 2024-02-01



#	Article	IF	CITATIONS
1	Effect of Mg doping on the electrical, dielectric and relaxation properties of LiMnPO4 nanoparticles. Indian Journal of Physics, 2022, 96, 1017-1023.	1.8	6
2	Biomassâ€derived ant colonyâ€like ion diffused redox porous carbon toward economical and highâ€performance quasiâ€solidâ€state supercapacitor. International Journal of Energy Research, 2022, 46, 1593-1608.	4.5	7
3	ZnO Nanoflakes Embedded Polymer Matrix for Highâ€Performance Mechanical Energy Harvesting. Advanced Materials Technologies, 2022, 7, 2100858.	5.8	4
4	Recent Advanced Development of Artificial Interphase Engineering for Stable Sodium Metal Anodes. Small, 2022, 18, e2102250.	10.0	46
5	Nitrogen―and carbonâ€rich <scp>Ni₂O₃</scp> nanolayer shielded <scp>Ni₃C</scp> elongated square bipyramidalâ€like nanostructures for hybrid supercapacitors. International Journal of Energy Research, 2022, 46, 4895-4907.	4.5	2
6	rGOâ€ZnSnO ₃ Nanostructureâ€Embedded Triboelectric Polymerâ€Based Hybridized Nanogenerators. Advanced Materials Technologies, 2022, 7, .	5.8	11
7	Unraveling CoNiP‒CoP ₂ 3Dâ€onâ€1D Hybrid Nanoarchitecture for Longâ€Lasting Electrochemical Hybrid Cells and Oxygen Evolution Reaction. Advanced Science, 2022, 9, e2104877.	11.2	26
8	Prussianâ€Blue Analogueâ€Derived Hollow Structured Co ₃ S ₄ /CuS ₂ /NiS ₂ Nanocubes as an Advanced Batteryâ€Type Electrode Material for Highâ€Performance Hybrid Supercapacitors. Small, 2022, 18, e2105185.	10.0	35
9	Hierarchical multi-metal-doped mesoporous NiO-silica nanoparticles towards a viable platform for Li-ion battery electrode application. Korean Journal of Chemical Engineering, 2022, 39, 1959-1967.	2.7	6
10	Facile synthesis of <scp> MgCo ₂ O ₄ </scp> hexagonal nanostructure via coâ€precipitation approach and its supercapacitive properties. International Journal of Energy Research, 2022, 46, 7788-7798.	4.5	5
11	Review on the recent progress in the nanocomposite polymer electrolytes on the performance of lithiumâ€ion batteries. International Journal of Energy Research, 2022, 46, 7137-7174.	4.5	11
12	Transition metal dichalcogenide nanostructured electrodes without calcination for aqueous asymmetric supercapacitors. International Journal of Energy Research, 2022, 46, 9414-9430.	4.5	7
13	An Efficient Power Management System Using Dynamically Configured Multiple Triboelectric Nanogenerators and Dualâ€Parameter Maximum Power Point Tracking. Advanced Energy Materials, 2022, 12, .	19.5	8
14	Highâ€Efficiency Poly(Vinylidene Fluorideâ€Coâ€Hexafluoropropylene) Loaded 3D Marigold Flowerâ€Like Bismuth Tungstate Triboelectric Films for Mechanical Energy Harvesting and Sensing Applications. Small, 2022, 18, e2200822.	10.0	10
15	Regulating Dendriteâ€Free Zinc Deposition by Red Phosphorousâ€Derived Artificial Protective Layer for Zinc Metal Batteries. Advanced Science, 2022, 9, e2200155.	11.2	41
16	Structural and electrochemical properties of mesoporous <scp> FeVO ₄ </scp> as a negative electrode for lithiumâ€ion battery. International Journal of Energy Research, 2022, 46, 13590-13601.	4.5	8
17	<scp> Mn ₂ V ₂ O ₇ </scp> spiked ballâ€ike material as bifunctional oxygen catalyst for zincâ€air batteries. International Journal of Energy Research, 2022, 46, 13528-13540.	4.5	3
18	High-sensitivity luminescent thermometer based on Mn4+/Sm3+ dual-emission centers in double-perovskite tellurate. Ceramics International, 2022, 48, 27664-27671	4.8	24

NARSIMLU DAULATABAD

#	Article	IF	CITATIONS
19	Cerium vanadate/carbon nanotube hybrid composite nanostructures as a high-performance anode material for lithium-ion batteries. Journal of Energy Chemistry, 2021, 58, 25-32.	12.9	34
20	Excellent photoluminescence and cathodoluminescence properties in Eu3+-activated Sr2LaNbO6 materials for multifunctional applications. Chemical Engineering Journal, 2021, 406, 127154.	12.7	113
21	Ternary MOF-Based Redox Active Sites Enabled 3D-on-2D Nanoarchitectured Battery-Type Electrodes for High-Energy-Density Supercapatteries. Nano-Micro Letters, 2021, 13, 17.	27.0	64
22	Electrochemical performance of SnO2 rods and SnO2/rGO, SnO2/MWCNTs composite materials as an anode for lithium-ion battery application-A comparative study. Journal of Materials Science: Materials in Electronics, 2021, 32, 7619-7629.	2.2	6
23	High capacity performance of <scp> NiCo ₂ O ₄ </scp> nanostructures as a binderâ€free anode material for <scp>lithiumâ€ion</scp> batteries. International Journal of Energy Research, 2021, 45, 13355-13364.	4.5	5
24	Y-ZnO Microflowers Embedded Polymeric Composite Films to Enhance the Electrical Performance of Piezo/Tribo Hybrid Nanogenerators for Biomechanical Energy Harvesting and Sensing Applications. ACS Sustainable Chemistry and Engineering, 2021, 9, 4600-4610.	6.7	22
25	Strong Green Emission of Erbium(III)-Activated La ₂ MgTiO ₆ Phosphors for Solid-State Lighting and Optical Temperature Sensors. ACS Sustainable Chemistry and Engineering, 2021, 9, 5105-5115.	6.7	55
26	Charge transfer band excitation of La ₃ NbO ₇ :Sm ³⁺ phosphors induced abnormal thermal quenching toward highâ€sensitivity thermometers. Journal of the American Ceramic Society, 2021, 104, 4065-4074.	3.8	21
27	Binderâ€free preparation of bimetallic oxide vertical nanosheet arrays toward highâ€rate performance and energy density supercapacitors. International Journal of Energy Research, 2021, 45, 13999-14009.	4.5	10
28	Three-dimensional flower-like nickel doped cobalt phosphate hydrate microarchitectures for asymmetric supercapacitors. Journal of Colloid and Interface Science, 2021, 592, 145-155.	9.4	22
29	Advantageous Occupation of Europium(III) in the B Site of Double-Perovskite Ca ₂ BBâ€2O ₆ (B = Y, Gd, La; Bâ€2 = Sb, Nb) Frameworks for White-Light-Emitting Diodes. ACS Sustainable Chemistry and Engineering, 2021, 9, 7960-7972.	6.7	30
30	Design and characteristics of lowâ€resistance lithiumâ€ion battery pack and its fast charging method for smart phones. International Journal of Energy Research, 2021, 45, 17631-17646.	4.5	4
31	Template and solâ€gel routed <scp> CoMn ₂ O ₄ </scp> nanofibers for supercapacitor applications. International Journal of Energy Research, 2021, 45, 19413-19422.	4.5	19
32	Nitrogenâ€doped reduced graphene oxide incorporated porous rodâ€like cobalt molybdate as an anode for highâ€capacity longâ€life lithiumâ€ion batteries. International Journal of Energy Research, 2021, 45, 19509-19520.	4.5	11
33	Oneâ€Pot Hydrothermalâ€Derived NiS ₂ –CoMo ₂ S ₄ with Vertically Aligned Nanorods as a Binderâ€Free Electrode for Coin ellâ€Type Hybrid Supercapacitor. Small Methods, 2021, 5, e2100335.	8.6	35
34	LiTaO ₃ -Based Flexible Piezoelectric Nanogenerators for Mechanical Energy Harvesting. ACS Applied Materials & Interfaces, 2021, 13, 46526-46536.	8.0	17
35	3D printed bidirectional rotatory hybrid nanogenerator for mechanical energy harvesting. Nano Energy, 2021, 88, 106250.	16.0	18
36	Microwave hydrothermal synthesis and electrochemical characterization of NiMoO4 nanosheets/SnO2 nanospheres/rGO nanocomposite as high-performance anode for lithium-ion batteries. Inorganic Chemistry Communication, 2021, 133, 108916.	3.9	5

#	Article	IF	CITATIONS
37	Tailoring the surface in copper manganese oxide materials and enhanced redox nature by graphitic carbon nitride sheets with ultra-long life for electrochemical applications. Journal of Materials Chemistry A, 2021, 9, 21448-21460.	10.3	4
38	Bifunctional application of La ₃ BWO ₉ :Bi ³⁺ ,Sm ³⁺ phosphors with strong orange-red emission and sensitive temperature sensing properties. Dalton Transactions, 2021, 50, 15187-15197.	3.3	18
39	Nanosilverâ€Particles Integrated Ni ₃ Sn ₂ S ₂ oS Composite as an Advanced Electrode for High Energy Density Hybrid Cell. Small Methods, 2021, 5, e2100907.	8.6	3
40	High coercivity in α-Fe2O3 nanostructures synthesized by surfactant-free microwave-assisted solvothermal method. Physics Letters, Section A: General, Atomic and Solid State Physics, 2020, 384, 126038.	2.1	9
41	Enhanced energy storage performance of nanocrystalline Sm-doped CoFe2O4 as an effective anode material for Li-ion battery applications. Journal of Solid State Electrochemistry, 2020, 24, 225-236.	2.5	12
42	lon and electron-conducting additive effect on Li-ion charge storage performance of CuFe2O4/SiO2 composite aerogel anode. Ceramics International, 2020, 46, 25330-25340.	4.8	5
43	β-NiS 3D micro-flower-based electrode for aqueous asymmetric supercapacitors. Sustainable Energy and Fuels, 2020, 4, 5550-5559.	4.9	20
44	Thermalâ€couple levels of ⁴ S _{3/2} and ² H _{11/2} in Na(Ca,) Tj E Journal of the American Ceramic Society, 2020, 103, 7082-7094.	TQq0 0 0 3.8	rgBT /Overloc 20
45	Metal–Organic Frameworkâ€Derived Co ₃ V ₂ O ₈ @CuV ₂ O ₆ Hybrid Architecture as a Multifunctional Binderâ€Free Electrode for Liâ€Ion Batteries and Hybrid Supercapacitors. Small, 2020, 16. e2003983.	10.0	68
46	Graphene Matrix Sheathed Metal Vanadate Porous Nanospheres for Enhanced Longevity and High-Rate Energy Storage Devices. ACS Applied Materials & Interfaces, 2020, 12, 27074-27086.	8.0	37
47	Integrated Design of Highly Porous Cellulose-Loaded Polymer-Based Triboelectric Films toward Flexible, Humidity-Resistant, and Sustainable Mechanical Energy Harvesters. ACS Energy Letters, 2020, 5, 2140-2148.	17.4	68
48	Evolution of Er3+/Yb3+-codoped NaGdF4 nanorods at room temperature for non-contact nanothermometer and optical heater. Applied Physics A: Materials Science and Processing, 2020, 126, 1.	2.3	5
49	Label-Free Surface-Enhanced Raman Spectroscopy Biosensor for On-Site Breast Cancer Detection Using Human Tears. ACS Applied Materials & Interfaces, 2020, 12, 7897-7904.	8.0	83
50	Rational design of SnO2 nanoflakes as a stable and high rate anode for lithium-ion batteries. Journal of Materials Science: Materials in Electronics, 2020, 31, 8556-8563.	2.2	2
51	Designing hierarchical NiCo2S4 nanospheres with enhanced electrochemical performance for supercapacitors. Journal of Solid State Electrochemistry, 2020, 24, 1033-1044.	2.5	6
52	Enhanced ionic conductivity of electrospun nanocomposite (PVDFâ€HFP + TiO 2 nanofibers fillers) polymer fibrous membrane electrolyte for DSSC application. Polymer Composites, 2019, 40, 1585-1594.	4.6	101
53	Multifunctional core-shell-like nanoarchitectures for hybrid supercapacitors with high capacity and long-term cycling durability. Nano Research, 2019, 12, 2597-2608.	10.4	31
54	Facile synthesis of MoO3/rGO nanocomposite as anode materials for high performance lithium-ion battery applications. Journal of Alloys and Compounds, 2019, 810, 151920.	5.5	39

#	Article	IF	CITATIONS
55	High-Efficiency and Thermally Sustainable Perovskite Solar Cells with Sandpaper-Aided Flexible Haze/Antireflective Films. ACS Sustainable Chemistry and Engineering, 2019, 7, 12981-12989.	6.7	11
56	Wearable Single-Electrode-Mode Triboelectric Nanogenerator via Conductive Polymer-Coated Textiles for Self-Power Electronics. ACS Sustainable Chemistry and Engineering, 2019, 7, 16450-16458.	6.7	109
57	High-performance quasi-solid-state asymmetric supercapacitors based on BiMn2O5 nanoparticles and redox-additive electrolytes. Inorganic Chemistry Frontiers, 2019, 6, 2061-2070.	6.0	12
58	Samarium(<scp>iii</scp>) and terbium(<scp>iii</scp>) ion-doped NaLa(MoO ₄) ₂ phosphors for versatile applications. New Journal of Chemistry, 2019, 43, 10645-10657.	2.8	34
59	Role of quercetin and caloric restriction on the biomolecular composition of aged rat cerebral cortex: An FTIR study. Spectrochimica Acta - Part A: Molecular and Biomolecular Spectroscopy, 2019, 220, 117128.	3.9	8
60	Electrospun Nanocomposite Ag–ZnO Nanofibrous Photoanode for Better Performance of Dye-Sensitized Solar Cells. Journal of Electronic Materials, 2019, 48, 4389-4399.	2.2	11
61	Rapid design of a core–shell-like metal hydroxide/oxide composite and activated carbon from biomass for high-performance supercapattery applications. Inorganic Chemistry Frontiers, 2019, 6, 1707-1720.	6.0	19
62	An Integrated Approach Toward Renewable Energy Storage Using Rechargeable Ag@Ni _{0.67} Co _{0.33} Sâ€Based Hybrid Supercapacitors. Small, 2019, 15, e1805418.	10.0	101
63	Nearâ€ultraviolet light–induced dazzling red emission in CaGd ₂ (MoO ₄) ₄ :2 <i>x</i> Sm ³⁺ compounds for phosphorâ€converted WLEDs. Journal of the American Ceramic Society, 2019, 102, 5353-5364.	3.8	40
64	Designing chain-like nickel pyro-vanadate porous spheres as an advanced electrode material for supercapacitors. Inorganic Chemistry Frontiers, 2019, 6, 1087-1096.	6.0	14
65	Facile preparation of Eu ³⁺ -activated Ca ₇ (VO ₄) ₄ O nanoparticles: a blue light-triggered red-emitting platform for indoor solid-state lighting. New Journal of Chemistry, 2019, 43, 6688-6695.	2.8	32
66	Oneâ€Pot Synthesis of Homogeneous EuF ₃ Nanoplates: A Nearâ€Ultraviolet Lightâ€Induced Redâ€Emitting Bifunctional Platform for in vitro Cell Imaging and Solidâ€State Lighting. ChemistrySelect, 2019, 4, 2275-2280.	1.5	3
67	Humidity Sustained Wearable Pouchâ€Type Triboelectric Nanogenerator for Harvesting Mechanical Energy from Human Activities. Advanced Functional Materials, 2019, 29, 1807779.	14.9	99
68	Streptavidin activated hydroxyl radicals enhanced photocatalytic and photoelectrochemical properties of membrane-bound like CaMoO ₄ :Eu ³⁺ hybrid structures. Journal of Materials Chemistry A, 2019, 7, 23105-23120.	10.3	19
69	Structural, electrical, and dielectric properties of nickel-doped spinel LiMn2O4 nanorods. lonics, 2019, 25, 981-990.	2.4	15
70	High conducting nanocomposite electrospun PVDF-HFP/ \$\$hbox {TiO}_{2}\$\$ TiO 2 quasi-solid electrolyte for dye-sensitized solar cell. Journal of Materials Science: Materials in Electronics, 2019, 30, 1199-1213.	2.2	23
71	Ba3P4O13:Eu3+ phosphors with high thermal stability and high internal quantum efficiency for near-ultraviolet white light-emitting diodes. Applied Physics A: Materials Science and Processing, 2019, 125, 1.	2.3	9
72	Conductivity and dielectric permittivity studies of Klâ€based nanocomposite (PEO/PMMA/KI/I ₂ /ZnO nanorods) polymer solid electrolytes. Polymer Composites, 2019, 40, 2919-2928.	4.6	26

#	Article	IF	CITATIONS
73	Structural characterization, electrical conductivity and open circuit voltage studies of the nanocrystalline La10Si6O27 electrolyte material for SOFCs. Applied Physics A: Materials Science and Processing, 2018, 124, 1.	2.3	7
74	Energy Back Transfer Induced Color Controllable Upconversion Emissions in La ₂ MoO ₆ :Er ³⁺ /Yb ³⁺ Nanocrystals for Versatile Applications. Particle and Particle Systems Characterization, 2018, 35, 1700416.	2.3	41
75	Electrospun Sn–SnO2/C composite nanofibers as an anode material for lithium battery applications. Journal of Materials Science: Materials in Electronics, 2018, 29, 11117-11123.	2.2	15
76	Synthesis of Er(III)/Yb(III)-doped BiF3 upconversion nanoparticles for use in optical thermometry. Mikrochimica Acta, 2018, 185, 237.	5.0	58
77	High-performance pouch-type hybrid supercapacitor based on hierarchical NiO-Co3O4-NiO composite nanoarchitectures as an advanced electrode material. Nano Energy, 2018, 48, 81-92.	16.0	251
78	Triboelectric nanogenerators with gold-thin-film-coated conductive textile as floating electrode for scavenging wind energy. Nano Research, 2018, 11, 101-113.	10.4	47
79	Utilizing Waste Cable Wires for Highâ€Performance Fiberâ€Based Hybrid Supercapacitors: An Effective Approach to Electronicâ€Waste Management. Advanced Energy Materials, 2018, 8, 1702201.	19.5	140
80	Surfactant-free microwave hydrothermal synthesis of SnO2 nanosheets as an anode material for lithium battery applications. Ceramics International, 2018, 44, 201-207.	4.8	38
81	Ultrafast synthesis of bifunctional Er3+/Yb3+-codoped NaBiF4 upconverting nanoparticles for nanothermometer and optical heater. Journal of Colloid and Interface Science, 2018, 514, 172-181.	9.4	167
82	Fallen leaves derived honeycomb-like porous carbon as a metal-free and low-cost counter electrode for dye-sensitized solar cells with excellent tri-iodide reduction. Journal of Colloid and Interface Science, 2018, 513, 843-851.	9.4	44
83	Hierarchically Designed Ag@Ce ₆ Mo ₁₀ O ₃₉ Marigold Flower-Like Architectures: An Efficient Electrode Material for Hybrid Supercapacitors. ACS Applied Materials & Interfaces, 2018, 10, 36976-36987.	8.0	40
84	Surfactant-free microwave-hydrothermal synthesis of SnO2 flower-like structures as an anode material for lithium-ion batteries. Materialia, 2018, 4, 276-281.	2.7	14
85	Enhanced electrochemical performance of MnCo2O4 nanorods synthesized via microwave hydrothermal method for supercapacitor applications. Journal of Materials Science: Materials in Electronics, 2018, 29, 21194-21204.	2.2	26
86	Near-Infrared Light-Triggered Visible Upconversion Emissions in Er ³⁺ /Yb ³⁺ -Codoped Y ₂ Mo ₄ O ₁₅ Microparticles for Simultaneous Noncontact Optical Thermometry and Solid-State Lighting. Industrial & Engineering Chemistry Research, 2018, 57, 13077-13086.	3.7	37
87	Enabling redox chemistry with hierarchically designed bilayered nanoarchitectures for pouch-type hybrid supercapacitors: A sunlight-driven rechargeable energy storage system to portable electronics. Nano Energy, 2018, 50, 448-461.	16.0	75
88	Shapeâ€Tunable Selective Synthesis of Bismuth Fluoride Nanostructures for Versatile Applications. Particle and Particle Systems Characterization, 2018, 35, 1800018.	2.3	8
89	Achieving a High Areal Capacity with a Binder-Free Copper Molybdate Nanocone Array-Based Positive Electrode for Hybrid Supercapacitors. Inorganic Chemistry, 2018, 57, 8440-8450.	4.0	30
90	Enhanced Performance of Microarchitectured PTFE-Based Triboelectric Nanogenerator via Simple Thermal Imprinting Lithography for Self-Powered Electronics. ACS Applied Materials & Interfaces, 2018, 10, 24181-24192.	8.0	87

#	Article	IF	CITATIONS
91	Microwave-assisted hydrothermal synthesis of SnO2/reduced graphene-oxide nanocomposite as anode material for high performance lithium-ion batteries. Journal of Materials Science: Materials in Electronics, 2018, 29, 14723-14732.	2.2	15
92	High Capacity Electrospun MgFe ₂ 0 ₄ –C Composite Nanofibers as an Anode Material for Lithium Ion Batteries. ChemistrySelect, 2018, 3, 8010-8017.	1.5	19
93	Enhancing the output performance of hybrid nanogenerators based on Al-doped BaTiO ₃ composite films: a self-powered utility system for portable electronics. Journal of Materials Chemistry A, 2018, 6, 16101-16110.	10.3	63
94	High-Performance Flexible Piezoelectric-Assisted Triboelectric Hybrid Nanogenerator via Polydimethylsiloxane-Encapsulated Nanoflower-like ZnO Composite Films for Scavenging Energy from Daily Human Activities. ACS Sustainable Chemistry and Engineering, 2018, 6, 8525-8535.	6.7	82
95	Rational design of forest-like nickel sulfide hierarchical architectures with ultrahigh areal capacity as a binder-free cathode material for hybrid supercapacitors. Journal of Materials Chemistry A, 2018, 6, 13178-13190.	10.3	82
96	Paper-Based Surface-Enhanced Raman Spectroscopy for Diagnosing Prenatal Diseases in Women. ACS Nano, 2018, 12, 7100-7108.	14.6	101
97	Microwave hydrothermal synthesis of α-MnMoO ₄ nanorods for high electrochemical performance supercapacitors. RSC Advances, 2018, 8, 22559-22568.	3.6	29
98	Cation Substitution Induced Enhanced Photoluminescence Properties of Gd _{2(1â^'} <i>_x</i> _{â^'} <i>_y</i> ₎ Y ₂ <i Phosphors for Indoor Lighting. Applied Science and Convergence Technology, 2018, 27, 52-55.</i 	> <aonap>x<!--</td--><td>sub>Mo<</td></aonap>	su b >Mo<
99	Optical, spectral, and thermal analyses of InGaN/GaN nearâ€ultraviolet flipâ€chip lightâ€emitting diodes with different package structures. Physica Status Solidi (A) Applications and Materials Science, 2017, 214, 1600741.	1.8	3
100	Broad near-ultraviolet and blue excitation band induced dazzling red emissions in Eu ³⁺ -activated Gd ₂ MoO ₆ phosphors for white light-emitting diodes. RSC Advances, 2017, 7, 3170-3178.	3.6	96
101	Broad red-emission of Sr ₃ Y ₂ Ge ₃ O ₁₂ :Eu ²⁺ garnet phosphors under blue excitation for warm WLED applications. RSC Advances, 2017, 7, 13281-13288.	3.6	52
102	Highly Reproducible Au-Decorated ZnO Nanorod Array on a Graphite Sensor for Classification of Human Aqueous Humors. ACS Applied Materials & Interfaces, 2017, 9, 5891-5899.	8.0	52
103	Upconversion emission and cathodoluminescence of Er3+-doped NaYbF4 nanoparticles for low-temperature thermometry and field emission displays. Applied Physics A: Materials Science and Processing, 2017, 123, 1.	2.3	10
104	Rare-earth free self-luminescent Ca2KZn2(VO4)3 phosphors for intense white light-emitting diodes. Scientific Reports, 2017, 7, 42348.	3.3	68
105	Conductive silver nanowires-fenced carbon cloth fibers-supported layered double hydroxide nanosheets as a flexible and binder-free electrode for high-performance asymmetric supercapacitors. Nano Energy, 2017, 36, 58-67.	16.0	291
106	Tunable color upconverison emissions in erbium(III)-doped BiOCl microplates for simultaneous thermometry and optical heating. Mikrochimica Acta, 2017, 184, 2661-2669.	5.0	39
107	Morphology-controlled facile surfactant-free synthesis of 3D flower-like BiOI:Eu ³⁺ or Tb ³⁺ microarchitectures and their photoluminescence properties. Journal of Materials Chemistry C, 2017, 5, 6880-6890.	5.5	17
108	Ultrathin nickel hydroxide nanosheet arrays grafted biomass-derived honeycomb-like porous carbon with improved electrochemical performance as a supercapacitive material. Scientific Reports, 2017, 7, 45201.	3.3	58

#	Article	IF	CITATIONS
109	Evolution of CaGd ₂ ZnO ₅ :Eu ³⁺ nanostructures for rapid visualization of latent fingerprints. Journal of Materials Chemistry C, 2017, 5, 4246-4256.	5.5	69
110	A facile drop-casting approach to nanostructured copper oxide-painted conductive woven textile as binder-free electrode for improved energy storage performance in redox-additive electrolyte. Journal of Materials Chemistry A, 2017, 5, 2224-2234.	10.3	55
111	Wearable Fabrics with Self-Branched Bimetallic Layered Double Hydroxide Coaxial Nanostructures for Hybrid Supercapacitors. ACS Nano, 2017, 11, 10860-10874.	14.6	259
112	Simultaneous phase and size manipulation in NaYF ₄ :Er ³⁺ /Yb ³⁺ upconverting nanoparticles for a non-invasion optical thermometer. New Journal of Chemistry, 2017, 41, 13855-13861.	2.8	54
113	Yb ³⁺ -Concentration dependent upconversion luminescence and temperature sensing behavior in Yb ³⁺ /Er ³⁺ codoped Gd ₂ MoO ₆ nanocrystals prepared by a facile citric-assisted sol–gel method. Inorganic Chemistry Frontiers, 2017, 4. 1987-1995.	6.0	138
114	Red and green colors emitting spherical-shaped calcium molybdate nanophosphors for enhanced latent fingerprint detection. Scientific Reports, 2017, 7, 11571.	3.3	53
115	Effect of device package on optical, spectral, and thermal properties of InGaN/GaN near-ultraviolet lateral light-emitting diodes. Journal of the Korean Physical Society, 2017, 71, 319-324.	0.7	1
116	Eu3+-activated La2MoO6-La2WO6 red-emitting phosphors with ultrabroad excitation band for white light-emitting diodes. Scientific Reports, 2017, 7, 11953.	3.3	58
117	Designed construction of yolk–shell structured trimanganese tetraoxide nanospheres via polar solvent-assisted etching and biomass-derived activated porous carbon materials for high-performance asymmetric supercapacitors. Journal of Materials Chemistry A, 2017, 5, 15808-15821.	10.3	57
118	Biomimetic nano/micro double-textured silicon with outstanding antireflective and super-hydrophilic surfaces for high optical performance. RSC Advances, 2017, 7, 33757-33763.	3.6	8
119	Largeâ€area growth of multiâ€layered MoS ₂ for violet (â^¼405 nm) photodetector applications Physica Status Solidi (A) Applications and Materials Science, 2017, 214, 1700221.	1.8	3
120	Photoluminescence, cathodoluminescence and thermal stability of Sm ³⁺ â€activated Sr ₃ La(VO ₄) ₃ redâ€emitting phosphors. Luminescence, 2017, 32, 1504-1510.	2.9	22
121	Synthesis, characterization and electrical properties of mesoporous nanocrystalline CoFe2O4 as a negative electrode material for lithium battery applications. Journal of Materials Science: Materials in Electronics, 2017, 28, 17208-17214.	2.2	12
122	Symbiotic organism search algorithm for simulation of J-V characteristics and optimizing internal parameters of DSSC developed using electrospun TiO2 nanofibers. Journal of Nanoparticle Research, 2017, 19, 1.	1.9	12
123	Metallic Layered Polyester Fabric Enabled Nickel Selenide Nanostructures as Highly Conductive and Binderless Electrode with Superior Energy Storage Performance. Advanced Energy Materials, 2017, 7, 1601362.	19.5	259
124	Metal-Semiconductor-Metal Near-Ultraviolet (~380Ânm) Photodetectors by Selective Area Growth of ZnO Nanorods and SiO2 Passivation. Nanoscale Research Letters, 2016, 11, 333.	5.7	28
125	Photoluminescence and cathodoluminescence properties of Sr2Gd8Si6O26:RE3+(RE3+=Tb3+or Sm3+) phosphors. Journal of Luminescence, 2016, 178, 183-191.	3.1	17
126	CH ₃ NH ₃ PbI ₃ planar perovskite solar cells with antireflection and self-cleaning function layers. Journal of Materials Chemistry A, 2016, 4, 7573-7579.	10.3	78

#	Article	IF	CITATIONS
127	Tunable emissions via the white region from Sr ₂ Gd ₈ (SiO ₄) ₆ O ₂ :RE ³⁺ (RE ³⁺ : Dy ³⁺ , Tm ³⁺ , Eu ³⁺) phosphors. New Journal of Chemistry, 2016, 40, 6214-6227.	2.8	24
128	Facile synthesis of Er ³⁺ /Yb ³⁺ -codoped NaYF ₄ nanoparticles: a promising multifunctional upconverting luminescent material for versatile applications. RSC Advances, 2016, 6, 94539-94546.	3.6	61
129	Thermal-tolerant polymers with antireflective and hydrophobic grooved subwavelength grating surfaces for high-performance optics. RSC Advances, 2016, 6, 79755-79762.	3.6	9
130	Hierarchical structured polymers for light-absorption enhancement of silicon-based solar power systems. RSC Advances, 2016, 6, 55159-55166.	3.6	13
131	Electrical and electrochemical studies of nanocrystalline mesoporous MgFe2O4 as anode material for lithium battery applications. Ceramics International, 2016, 42, 16789-16797.	4.8	42
132	Temperatureâ€dependent optical, spectral, and thermal characteristics of InGaN/GaN nearâ€ultraviolet lightâ€emitting diodes. Physica Status Solidi (A) Applications and Materials Science, 2016, 213, 46-51.	1.8	7
133	An Ultrahighâ€Performance Photodetector based on a Perovskite–Transitionâ€Metalâ€Dichalcogenide Hybrid Structure . Advanced Materials, 2016, 28, 7799-7806.	21.0	242
134	Controlled synthesis of yttrium gallium garnet spherical nanostructures modified by silver oxide nanoparticles for enhanced photocatalytic properties. CrystEngComm, 2016, 18, 8915-8925.	2.6	10
135	Birnessite-type MnO ₂ nanosheet arrays with interwoven arrangements on vapor grown carbon fibers as hybrid nanocomposites for pseudocapacitors. Dalton Transactions, 2016, 45, 19322-19328.	3.3	28
136	Hybrid Energy Cell with Hierarchical Nano/Micro-Architectured Polymer Film to Harvest Mechanical, Solar, and Wind Energies Individually/Simultaneously. ACS Applied Materials & Interfaces, 2016, 8, 30165-30175.	8.0	46
137	Effect of PMMA blend and ZnAl ₂ O ₄ fillers on ionic conductivity and electrochemical performance of electrospun nanocomposite polymer blend fibrous electrolyte membranes for lithium batteries. RSC Advances, 2016, 6, 6486-6495.	3.6	18
138	A facile one-step approach to hierarchically assembled core–shell-like MnO2@MnO2 nanoarchitectures on carbon fibers: An efficient and flexible electrode material to enhance energy storage. Nano Research, 2016, 9, 1507-1522.	10.4	98
139	Enhanced electrochemical performance of carbon-coated LiMPO4 (MÂ=ÂCo and Ni) nanoparticles as cathodes for high-voltage lithium-ion battery. Journal of Solid State Electrochemistry, 2016, 20, 1855-1863.	2.5	19
140	Synthesis and luminescent properties of red-emitting Eu3+-activated Ca0.5Sr0.5MoO4 phosphors. Journal of Materials Science, 2016, 51, 5427-5435.	3.7	38
141	Eu ³⁺ ion concentration induced 3D luminescence properties of novel red-emitting Ba ₄ La ₆ (SiO ₄)O:Eu ³⁺ oxyapatite phosphors for versatile applications. Journal of Materials Chemistry C, 2016, 4, 1039-1050.	5.5	63
142	A multifunctional hierarchical nano/micro-structured silicon surface with omnidirectional antireflection and superhydrophilicity via an anodic aluminum oxide etch mask. RSC Advances, 2016, 6, 3764-3773.	3.6	25
143	Highly efficient low temperature solution processable planar type CH ₃ NH ₃ PbI ₃ perovskite flexible solar cells. Journal of Materials Chemistry A, 2016, 4, 1572-1578.	10.3	223
144	Hierarchical Ni–Co layered double hydroxide nanosheets entrapped on conductive textile fibers: a cost-effective and flexible electrode for high-performance pseudocapacitors. Nanoscale, 2016, 8, 812-825.	5.6	327

#	Article	IF	CITATIONS
145	Synthesis, characterization and conductivity studies of ZnFe2O4 nanoparticles. AIP Conference Proceedings, 2015, , .	0.4	1
146	Structural and ionic conductivity studies of electrospun polymer blend P(VdF-co-HFP)/PMMA electrolyte membrane for lithium battery application. AIP Conference Proceedings, 2015, , .	0.4	0
147	Ba ₃ (PO ₄) ₂ hierarchical structures: synthesis, growth mechanism and luminescence properties. CrystEngComm, 2015, 17, 4647-4653.	2.6	18
148	Luminescence properties of Dy3+ ions activated novel warm white-light emitting CaGd2ZnO5 nanophosphors. Ceramics International, 2015, 41, 11228-11233.	4.8	22
149	Synthesis of nanocrystalline LiCoO ₂ powders by polymeric combustion process: an investigation on the effect of different carboxylic acids as fuel. International Journal of Higher Education Management, 2015, 1, 105-112.	1.3	5
150	Surface modification and characterization of nanocrystalline LiNi _{0.5} Co _{0.5} VO ₄ with Dy ₂ O ₃ by polymeric resin process. International Journal of Higher Education Management, 2015, 1, 100-104.	1.3	0
151	Strongly enhanced emission of terahertz radiation from nanostructured Ge surfaces. , 2015, , .		0
152	Broadband and wide-angle antireflective characteristics of nanoporous anodic alumina films for silicon-based optoelectronic applications. Applied Physics B: Lasers and Optics, 2015, 118, 439-447.	2.2	9
153	UV-A and UV-B excitation region broadened novel green color-emitting CaGd ₂ ZnO ₅ :Tb ³⁺ nanophosphors. RSC Advances, 2015, 5, 22217-22223.	3.6	38
154	Novel rare-earth-free yellow Ca5Zn3.92In0.08(V0.99Ta0.01O4)6 phosphors for dazzling white light-emitting diodes. Scientific Reports, 2015, 5, 10296.	3.3	73
155	Antireflective gradient-refractive-index material-distributed microstructures with high haze and superhydrophilicity for silicon-based optoelectronic applications. RSC Advances, 2015, 5, 25616-25624.	3.6	11
156	A.C conductivity and dielectric properties of spinel LiMn2O4 nanorods. Ceramics International, 2015, 41, 14070-14077.	4.8	38
157	Solar power generation enhancement of dye-sensitized solar cells using hydrophobic and antireflective polymers with nanoholes. RSC Advances, 2015, 5, 61284-61289.	3.6	22
158	Dual-enhancement of photoluminescence and cathodoluminescence in Eu ³⁺ -activated SrMoO ₄ phosphors by Na ⁺ doping. RSC Advances, 2015, 5, 60121-60127.	3.6	78
159	Strong Photocurrent Enhancements in Plasmonic Organic Photovoltaics by Biomimetic Nanoarchitectures with Efficient Light Harvesting. ACS Applied Materials & Interfaces, 2015, 7, 6706-6715.	8.0	31
160	Electrochemical Characterization of Electrospun Nanocomposite Polymer Blend Electrolyte Fibrous Membrane for Lithium Battery. Journal of Physical Chemistry B, 2015, 119, 5299-5308.	2.6	26
161	Rapid microwave assisted hydrothermal synthesis of porous α-Fe ₂ O ₃ nanostructures as stable and high capacity negative electrode for lithium and sodium ion batteries. RSC Advances, 2015, 5, 34761-34768.	3.6	50
162	Highly flexible conductive fabrics with hierarchically nanostructured amorphous nickel tungsten tetraoxide for enhanced electrochemical energy storage. Nano Research, 2015, 8, 3749-3763.	10.4	65

#	Article	IF	CITATIONS
163	La(OH) ₃ :Eu ³⁺ and La ₂ O ₃ :Eu ³⁺ nanorod bundles: growth mechanism and luminescence properties. CrystEngComm, 2015, 17, 9431-9442.	2.6	39
164	Multifunctional polymers with biomimetic compound architectures via nanoporous AAO films for efficient solar energy harvesting in dye-sensitized solar cells. RSC Advances, 2015, 5, 90103-90110.	3.6	16
165	Hydrothermal Synthesis and Photocatalytic Property of β-Ga2O3 Nanorods. Nanoscale Research Letters, 2015, 10, 364.	5.7	84
166	Synthesis and luminescent properties of CaLa2ZnO5:Ln (Ln:Tm3+ or Er3+) phosphors. Ceramics International, 2015, 41, 13264-13270.	4.8	16
167	Highly Transparent and Flexible Triboelectric Nanogenerators with Subwavelength-Architectured Polydimethylsiloxane by a Nanoporous Anodic Aluminum Oxide Template. ACS Applied Materials & Interfaces, 2015, 7, 20520-20529.	8.0	83
168	Multi-stacked PDMS-based triboelectric generators with conductive textile for efficient energy harvesting. RSC Advances, 2015, 5, 6437-6442.	3.6	50
169	Artificial inverted compound eye structured polymer films with light-harvesting and self-cleaning functions for encapsulated III–V solar cell applications. RSC Advances, 2015, 5, 60804-60813.	3.6	31
170	Optical performance improvement of semi-transparent metal film electrodes with biomimetic subwavelength gratings for high-performance optoelectronic device applications. RSC Advances, 2015, 5, 84865-84871.	3.6	6
171	Structural, electrical and dielectric properties of spinel type MgAl2O4 nanocrystalline ceramic particles synthesized by the gel-combustion method. Ceramics International, 2015, 41, 3178-3185.	4.8	51
172	Broadband and omnidirectional highly-transparent coverglasses coated with biomimetic moth-eye nanopatterned polymer films for solar photovoltaic system applications. Solar Energy Materials and Solar Cells, 2015, 134, 45-53.	6.2	82
173	Facile fabrication and characterization of arch-shaped triboelectric nanogenerator with a graphite top electrode. Physica Status Solidi (A) Applications and Materials Science, 2015, 212, 401-405.	1.8	16
174	Electrospun nanocomposite fibrous polymer electrolyte for secondary lithium battery applications. AIP Conference Proceedings, 2014, , .	0.4	4
175	Enhanced Device Efficiency of Bilayered Inverted Organic Solar Cells Based on Photocurable P3HTs with a Lightâ€Harvesting ZnO Nanorod Array. Advanced Energy Materials, 2014, 4, 1301338.	19.5	38
176	Structural characterization and electrical conductivity studies of BaMoO4 nanofibers prepared by sol–gel and electrospinning techniques. Journal of Sol-Gel Science and Technology, 2014, 72, 480-489.	2.4	23
177	Temperature- and size-dependent characteristics in ultrathin inorganic light-emitting diodes assembled by transfer printing. Applied Physics Letters, 2014, 104, .	3.3	35
178	Novel orange and reddish-orange color emitting BaGd2O4:Sm3+ nanophosphors by solvothermal reaction for LED and FED applications. Spectrochimica Acta - Part A: Molecular and Biomolecular Spectroscopy, 2014, 124, 383-388.	3.9	23
179	Structural, electrical and dielectric studies of nanocrystalline LiMnPO4 particles. Ionics, 2014, 20, 927-934.	2.4	18
180	Efficiency Enhancement of Organic Solar Cells Using Hydrophobic Antireflective Inverted Mothâ€Eye Nanopatterned PDMS Films. Advanced Energy Materials, 2014, 4, 1301315.	19.5	151

#	Article	IF	CITATIONS
181	Nanostructured encapsulation coverglasses with wide-angle broadband antireflection and self-cleaning properties for III–V multi-junction solar cell applications. Solar Energy Materials and Solar Cells, 2014, 120, 555-560.	6.2	42
182	Characterization and Electrochemical Properties of P(VdFâ€ <i>co</i> â€HFP) Based Electrospun Nanocomposite Fibrous Polymer Electrolyte Membrane for Lithium Battery Applications. Electroanalysis, 2014, 26, 2373-2379.	2.9	20
183	Self-assembled hierarchical β-cobalt hydroxide nanostructures on conductive textiles by one-step electrochemical deposition. CrystEngComm, 2014, 16, 11027-11034.	2.6	46
184	Binder effect on the battery performance of mesoporous copper ferrite nanoparticles with grain boundaries as anode materials. RSC Advances, 2014, 4, 44089-44099.	3.6	22
185	High transparency and triboelectric charge generation properties of nano-patterned PDMS. RSC Advances, 2014, 4, 10216.	3.6	60
186	Concentration and penetration depth dependent tunable emissions from Eu ³⁺ co-doped SrY ₂ O ₄ :Dy ³⁺ nanocrystalline phosphor. New Journal of Chemistry, 2014, 38, 163-169.	2.8	77
187	Pump power induced tunable upconversion emissions from Er ³⁺ /Tm ³⁺ /Yb ³⁺ ions tri-doped SrY ₂ O ₄ nanocrystalline phosphors. New Journal of Chemistry, 2014, 38, 3413.	2.8	24
188	Theoretical modeling and optimization of Ill–V GaInP/GaAs/Ge monolithic triple-junction solar cells. Journal of the Korean Physical Society, 2014, 64, 1561-1565.	0.7	20
189	Electrical and dielectric properties of rare earth oxides coated LiCoO2 particles. Ionics, 2014, 20, 175-181.	2.4	25
190	Efficiency improvement of Ill–V GaAs solar cells using biomimetic TiO2 subwavelength structures with wide-angle and broadband antireflection properties. Solar Energy Materials and Solar Cells, 2014, 127, 43-49.	6.2	45
191	Effect of ZnO filler concentration on the conductivity, structure and morphology of PVdF-HFP nanocomposite solid polymer electrolyte for lithium battery application. Ionics, 2013, 19, 1835-1842.	2.4	46
192	Efficient piezoelectric ZnO nanogenerators based on Au-coated silica sphere array electrode. Nanoscale Research Letters, 2013, 8, 511.	5.7	3
193	Design and fabrication of antireflective GaN subwavelength grating structures using periodic silica sphere monolayer array patterning. Applied Physics B: Lasers and Optics, 2013, 113, 567-573.	2.2	9
194	Effects of point defect healing on phosphorus implanted germanium n+/p junction and its thermal stability. Journal of Applied Physics, 2013, 114, .	2.5	4
195	Solvothermal synthesis and luminescent properties of Y ₂ Ti ₂ O ₇ Eu ³⁺ spheres. Physica Status Solidi - Rapid Research Letters, 2013, 7, 224-227.	2.4	19
196	Enhanced conductivity and electrical relaxation studies of carbon-coated LiMnPO4 nanorods. lonics, 2013, 19, 461-469.	2.4	20
197	Dropâ€cast and dyeâ€sensitized ZnO nanorodâ€based visibleâ€light photodetectors. Physica Status Solidi - Rapid Research Letters, 2013, 7, 659-663.	2.4	7
198	Preparation of ZnO nanorods on cellulose fiber paper and their chargeâ€generating application for waste paper recycling. Physica Status Solidi - Rapid Research Letters, 2013, 7, 985-988.	2.4	6

#	Article	IF	CITATIONS
199	Characteristics of terahertz pulses from antireflective GaAs surfaces with nanopillars. Journal of Applied Physics, 2013, 113, .	2.5	5
200	Synthesis and luminescent properties of nanocrystalline CaYAlO ₄ :Sm ³⁺ phosphors. Physica Status Solidi (B): Basic Research, 2013, 250, 374-377.	1.5	12
201	Optical studies of ZnO nanoparticles and 1-D nanofibers. AIP Conference Proceedings, 2013, , .	0.4	1
202	Temperature and injection current dependent optical and thermal characteristics of InGaN-based green large-area light-emitting diodes. Physica Status Solidi (A) Applications and Materials Science, 2013, 210, 2479-2484.	1.8	5
203	Enhanced Light Extraction of GaN-Based Green Light-Emitting Diodes With GaOOH Rods. IEEE Photonics Technology Letters, 2012, 24, 285-287.	2.5	6
204	Light Output Extraction Enhancement in GaN-Based Green LEDs With Periodic AZO Subwavelength Nanostructure Arrays. IEEE Photonics Technology Letters, 2012, 24, 1381-1383.	2.5	7
205	Formation of Ca ₂ Gd ₈ (SiO ₄) ₆ O ₂ Nanorod Bundles Based on Crystal Splitting by Mixed Solvothermal and Hydrothermal Reaction Methods. Crystal Growth and Design, 2012, 12, 960-969.	3.0	45
206	Mesoporous and hierarchical manganese dioxide nanoplates/nanowalls on Ni/PET conductive fabric. Physica Status Solidi - Rapid Research Letters, 2012, 6, 385-387.	2.4	1
207	Optimization of THz semi-insulating surface plasmon waveguide structures of GaSb/AlSb quantum cascade lasers. Journal of the Korean Physical Society, 2012, 61, 1365-1369.	0.7	2
208	A facile and efficient strategy for the preparation of stable CaMoO4 spherulites using ammonium molybdate as a molybdenum source and their excitation induced tunable luminescent properties for optical applications. Journal of Materials Chemistry, 2012, 22, 15562.	6.7	97
209	Silver nanoparticle decorated ZnO nanorod arrays on AZO films for light absorption enhancement. Physica Status Solidi (A) Applications and Materials Science, 2012, 209, 297-301.	1.8	16
210	Characteristics and simulation analysis of GaNâ€based vertical light emitting diodes via waferâ€level additional surface roughening process. Physica Status Solidi (A) Applications and Materials Science, 2012, 209, 1168-1173.	1.8	2
211	Diffuse lightâ€scattering properties of nanocracked and porous MoO ₃ films selfâ€formed by electrodeposition and thermal annealing. Physica Status Solidi (A) Applications and Materials Science, 2012, 209, 2161-2166.	1.8	6
212	Facile fabrication of forestâ€like ZnO hierarchical structures on conductive fabric substrate. Physica Status Solidi - Rapid Research Letters, 2012, 6, 355-357.	2.4	8
213	Tunable growth of urchin-shaped ZnO nanostructures on patterned transparent substrates. CrystEngComm, 2012, 14, 5824.	2.6	9
214	Photoluminescence and Cathodoluminescence Properties of Nanocrystalline <scp><scp>Ca₂Gd₈Si₆O₂₆</scp></scp> :< Journal of the American Ceramic Society, 2012, 95, 238-242.	scp 3. &scp>	∘Smsasup>3+<
215	Thermal characteristics of InP-based mid-infrared quantum cascade lasers at λ â^1⁄4 8.8 µm. Journal of the Korean Physical Society, 2012, 60, 1757-1761.	0.7	0
216	Three-dimensional lithium manganese phosphate microflowers for lithium-ion battery applications.	2.9	11

Journal of Applied Electrochemistry, 2012, 42, 163-167.

NARSIMLU DAULATABAD

#	Article	IF	CITATIONS
217	Strong Light-Extraction Enhancement of GaN-Based Light-Emitting Diodes with Top and Sidewall GaOOH Nanorod Arrays. Japanese Journal of Applied Physics, 2012, 51, 102102.	1.5	2
218	Light-Extraction Enhancement of Large-Area GaN-Based LEDs With Electrochemically Grown ZnO Nanorod Arrays. IEEE Photonics Technology Letters, 2011, 23, 1204-1206.	2.5	15
219	Preparation, characterization and electrical conductivity studies of nanocrystalline La doped BaMoO4. Materials Research Bulletin, 2011, 46, 32-41.	5.2	18
220	Preparation and characterization of nanocrystalline CoFe2O4 deposited on SiO2: in situ sol–gel process. Journal of Sol-Gel Science and Technology, 2011, 58, 24-32.	2.4	13
221	Influence of obliqueâ€angle sputtered transparent conducting oxides on performance of Siâ€based thin film solar cells. Physica Status Solidi (A) Applications and Materials Science, 2011, 208, 2220-2225.	1.8	12
222	Influence of etching process parameters on the antireflection property of Si SWSs by thermally dewetted Ag and Ag/SiO ₂ nanopatterns. Physica Status Solidi (A) Applications and Materials Science, 2011, 208, 1902-1907.	1.8	3
223	Analysis and design of waveguide structures for InGaAs/InAlAs quantum cascade lasers at <i>λ</i> â^¼â€‰4.6–9.5 µm. Physica Status Solidi (A) Applications and Materials Science, 2011, 2	:08 <mark>1.8</mark> 900-	2966.
224	Optical absorption enhancement of embedded Ag nanoparticles with ZnO nanorod arrays. Physica Status Solidi (A) Applications and Materials Science, 2011, 208, 2778-2782.	1.8	6
225	Design optimization of quantum cascade laser structures at <i>λ</i> â^¼â€‰11–12 µm. Physica S Applications and Materials Science, 2010, 207, 2190-2197.	Status Soli 1.8	di (A)
226	Synthesis of SiO[sub 2]â^•CoFe[sub 2]O[sub 4] nanocomposite by Base Catalyst Assisted In-situ Sol-Gel Process. , 2010, , .		1
227	1.3-\$mu\$m Laterally Tapered Ridge Waveguide DFB Lasers With Second-Order Cr Surface Gratings. IEEE Photonics Technology Letters, 2010, , .	2.5	2
228	Design and fabrication of nanoscale antireflection structures with linearly graded refractive index. , 2010, , .		0
229	Theoretical analysis of polarization characteristics of InGaN/GaN LEDs with photonic crystals. , 2009, , .		Ο
230	High-Performance Continuous-Wave Operation of \$lambda sim {hbox {4.6}}~mu{hbox {m}}\$ Quantum-Cascade Lasers Above Room Temperature. IEEE Journal of Quantum Electronics, 2008, 44, 747-754.	1.9	34
231	Coupling coefficient calculaltion of laterally coupled distributed feedback laser structure with metal surface gratings. , 2008, , .		2
232	AC Conductivity and Electrical Modulus Studies on Lithium Vanadophosphate Glasses. Journal of the American Ceramic Society, 2007, 90, 125-131.	3.8	20
233	Preparation and characterization of nanocrystallite size cuprous oxide. Materials Research Bulletin, 2007, 42, 1619-1624.	5.2	58
234	Preparation of NiAl2O4/SiO2 and Co2+-Doped NiAl2O4/SiO2 Nanocomposites by the Sol-Gel Route. Journal of the American Ceramic Society, 2006, 89, 060427083300002-???.	3.8	5

#	ARTICLE	IF	CITATIONS
235	Preparation, characterization and conductivity studies of AgI-Ag ₂ O-(TeO ₂ +) Tj ETQq1 1 1717-1720.	0.784314 3.7	rgBT /Ove 6
236	A.c. conductivity studies on the silver molybdo-arsenate glassy system. Journal of Materials Science, 1996, 31, 5471-5477.	3.7	17
237	Facile Hydrothermal Synthesis and Electrochemical Properties of CaMoO ₄ Nanoparticles for Aqueous Asymmetric Supercapacitors. ACS Sustainable Chemistry and Engineering, 0, , .	6.7	9
238	Effects of activated Sr 2+ ion content on strong blueâ€emitting Ca 2 Sb 2 O 7 materials for highâ€quality WLED devices. International Journal of Energy Research, 0, , .	4.5	4
239	Carbonâ€embedded mesoporous transition multimetal oxide nanospheres for longâ€lasting hybrid cells. International Journal of Energy Research, 0, , .	4.5	0